

# Hydrogen Exchange Study of DNA Duplexes Containing the Consensus Binding Site for *Arabidopsis thaliana* SPL14 Transcription Factor

Minjee Jeong,<sup>a</sup> Jin-Wan Park,<sup>a</sup> Hee-Eun Kim, Ju-Yong Lee, Ae-Ree Lee, Yong-Geun Choi, and Joon-Hwa Lee\*

Department of Chemistry and RINS, Gyeongsang National University, Jinju, Gyeongnam 660-701, Korea

\*E-mail: joonhwa@gnu.ac.kr

Received April 12, 2013, Accepted May 20, 2013

**Key Words :** NMR, Hydrogen exchange, SPL14 transcription factor, Arabidopsis, Base-pair stability

In plants, programmed cell death (PCD) is required for proper growth and tracheary element differentiation.<sup>1-4</sup> PCD also plays the important role in the plant defense against pathogen attack.<sup>5,6</sup> Mis-expression of *Arabidopsis thaliana* SPL14 (AtSPL14) gene affects resistance to PCD and modification of plant architecture.<sup>7</sup> AtSPL14 is a DNA-binding transcription factor, including a Cys- and His-rich SQUAMOSA promoter binding protein (SBP) domain.<sup>8</sup> SBP is defined as a conserved approximately 80 amino acid domain.<sup>8</sup> SBPs have roles in plant growth, metal sensing in algae, and directing development of leaves, embryos, and floral organs.<sup>7</sup> However, the molecular basis on the physiological functions of AtSPL14 in regulating plant PCD and/or development is not completely understood. NMR structures of SBP domains indicate that SBP forms a unique DNA-binding domain consisting of two Zn-finger structures.<sup>9,10</sup> Recently, the DNA consensus sequence (GTAC) for AtSPL14 binding was identified by systematic evolution of ligands by exponential enrichment (SELEX) or random binding site selection.<sup>8</sup> It was reported that the GTAC consensus sequence required one or two additional flanking nucleotides for effective AtSPL14-DNA interaction.<sup>8</sup>

Thus, it was thought to be that the minimum consensus DNA sequence for effective AtSPL14-DNA interaction is 5'-C<sup>1</sup>C<sup>2</sup>G<sup>3</sup>T<sup>4</sup>A<sup>5</sup>C<sup>6</sup>R<sup>7</sup>-3' (where R is A or G).<sup>8</sup> EMSA competition assays with various DNA sequences found that the point mutation at position 2-6 of the consensus sequence (5'-C<sup>1</sup>C<sup>2</sup>G<sup>3</sup>T<sup>4</sup>A<sup>5</sup>C<sup>6</sup>R<sup>7</sup>-3') significantly decreased the DNA binding affinity of AtSPL14, whereas the C-to-A and C-to-T mutation at position 1 of the consensus sequence did not affect.<sup>8</sup> To understand the DNA binding mechanism of AtSPL14 protein, the imino proton exchange rates were measured for the DNA duplex containing the consensus DNA-binding site for the AtSPL14 transcription factor (referred to as wt-SPL14 duplex, Fig. 1). To further understand the correlation between the base pair stability/dynamics and DNA binding affinity of the AtSPL14, the exchange rate constants of the imino protons for the wt-SPL14 duplex were compared with those of the mutant SPL14 duplexes (see Fig. 1), which display different binding affinities for AtSPL14 protein.

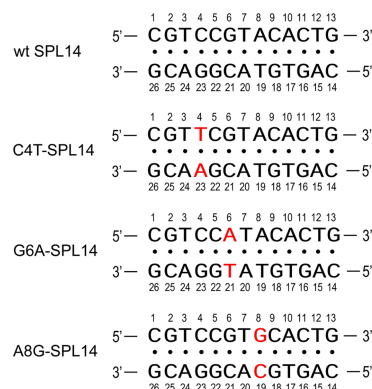


**Figure 1.** DNA sequence contexts of the wt-, C4T-, G6A-, and A8G-SPL14 DNA duplexes.

## Experimental Section

All DNA oligonucleotides were purchased from M-bio-tech Co. (Seoul, Korea). The oligonucleotides were purified by reverse-phase HPLC and desalted by Sephadex G-25 column. DNA duplexes were prepared by dissolving two strands at a 1:1 stoichiometric ratio in an NMR buffer (90% H<sub>2</sub>O/10% D<sub>2</sub>O solution containing 10 mM sodium phosphate (pH 8.0) and 100 mM NaCl). NMR experiments were carried out on a Agilent DD2 700 MHz spectrophotometer (GNU, Jinju) equipped with x,y,z-axis pulsed-field gradient cold probe. 1D NMR data were processed and analyzed with the program FELIX (Accelrys, San Diego, CA) or VNMRJ (Agilent, Santa Clara, CA) and 2D data were processed with the program NMRPIPE<sup>11</sup> and analyzed with the program Sparky.<sup>12</sup> To measure the hydrogen exchange rates of the imino protons, water magnetization transfer experiments were performed using delay times ranging from 5 to 100 ms.<sup>13</sup> The imino hydrogen exchange rate constants ( $k_{ex}$ ) were determined by fitting the data to Eq. (1):<sup>13</sup>

$$\frac{I(t)}{I_0} = 1 - 2 \frac{k_{ex}}{(R_{1w} - R_{1a})} (e^{-R_{1a}t} - e^{-R_{1w}t}) \quad (1)$$

where  $R_{1a}$  and  $R_{1w}$  were the independently measured and are the apparent longitudinal relaxation rates of the imino proton and water, respectively, and  $I_0$  and  $I(t)$  are the peak intensities of the imino proton in the water magnetization transfer experiments at times zero and  $t$ , respectively.<sup>13</sup>

<sup>a</sup>These authors contributed equally to this work.

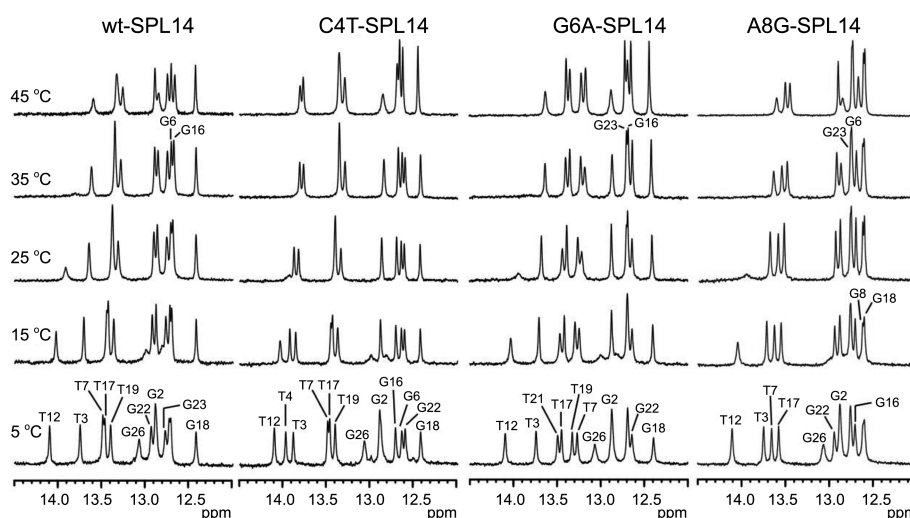


**Figure 2.** Temperature dependence of the imino proton resonances of the  $^1\text{H}$ -NMR spectra for the wt-, C4T-, G6A-, and A8G-SPL14 duplexes. The experimental temperatures are shown on the left of each spectrum.

## Results and Discussion

Two-dimensional NOESY spectra of the wt-, C4T-, G6A-, and A8G-SPL14 SPL14 duplexes in 90%  $\text{H}_2\text{O}/10\%$   $\text{D}_2\text{O}$  buffer solution containing 10 mM sodium phosphate (pH 8.0) and 100 mM NaCl were acquired at 15 °C with 120 and 250 ms mixing times. The imino proton resonances were assigned by the strong G-imino to C-amino or T-imino to A-H2 NOE cross peaks in the NOESY spectra. Figure 2 shows temperature-dependent imino proton spectra of the wt-, C4T-, G6A-, and A8G-SPL14 duplexes. In the wt-SPL14 duplex, all imino proton resonances except the terminal G13 imino proton resonance were observed at 5 °C. The T12 imino proton resonance was broadened at 25 °C and then disappeared as temperature was increased up to 35 °C, indicating instability of the T12·A15 base pair (Fig. 2). Most imino proton resonances except the T12 and terminal G12 and G26 were observed up to 45 °C, indicating that the wt-SPL14 duplex is relatively stable at  $\leq 45$  °C.

The exchange rate constants of the imino protons for the wt-SPL14 duplex were determined by water magnetization transfer method at 25 °C. Some protons show large differences in peak intensities as a function of delay time after

water inversion (Fig. 3). For example, rapid exchanging imino protons such as T12 show negative peaks at short delay times (20 ms in Fig. 3(a)), whereas the G22 resonance, which is the slowest exchanging imino proton, shows still positive up to 100 ms. The relative peak intensities of the water magnetization transfer for the imino proton resonances of the wt-SPL14 duplex at 25 °C are plotted as a function of delay time in Figure 3(b). Figure 3(c) shows the  $k_{\text{ex}}$  data of the imino protons of the wt-SPL14 duplex determined by fitting to Eq. (1). The G23, G22, and G18 imino protons are the slowly exchanging protons ( $k_{\text{ex}}$  of  $\sim 0.2 \text{ s}^{-1}$ ), indicating that the C4·G23, C5·G22, and C9·G18 base pairs are relatively very stable in the wt-SPL14 duplex. The T12 imino proton next to the terminal base pair shows severely broadening signal and has the largest exchange rate constant of any non-terminal base pairs ( $k_{\text{ex}}$  of  $49.6 \pm 5.1 \text{ s}^{-1}$ ). The G2 and T3 imino protons, which are two imino protons next to the other terminal base pairs, have the  $k_{\text{ex}}$  values of  $1.6 \pm 0.6 \text{ s}^{-1}$  and  $7.1 \pm 0.8 \text{ s}^{-1}$ , respectively.

Figure 4 shows the temperature-dependence of the  $k_{\text{ex}}$  values of the imino protons for the wt-SPL14 duplex. No significant changes in the  $k_{\text{ex}}$  values for the G imino protons of the stable C4·G22, C5·G23, and C9·G18 base pairs are

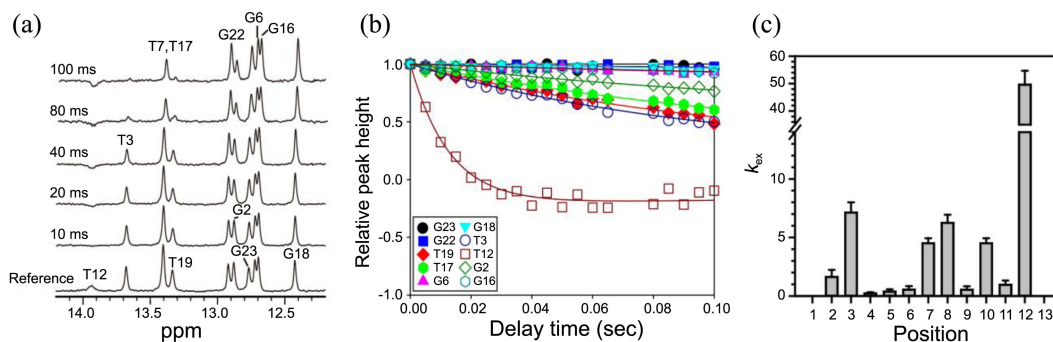


**Figure 3.** (a) 1D imino proton spectra of the water magnetization transfer experiments for the wt-SPL14 duplex at 25 °C. The delay times between the selective water inversion and acquisition pulse are indicated on the left of spectra. (b) Relative peak height  $[I(t)/I_0]$  in the water magnetization transfer spectra for the imino protons as a function of delay time. Solid lines indicate the best fitting of these data using Eq. (1). (c) The exchange rate constants of the imino protons for the wt-SPL14 duplex at 25 °C and the error bars represents fitting errors.

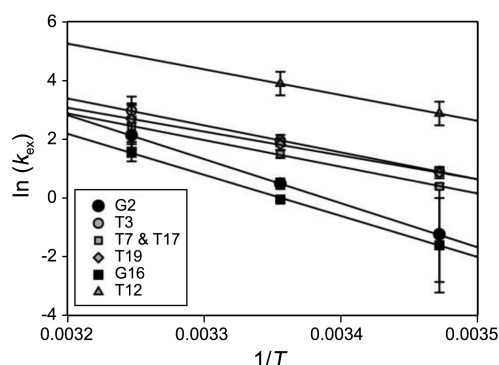


**Figure 4.** Logarithm scale of the  $k_{\text{ex}}$  values for the imino protons of wt-SPL14 duplex versus the inverse of temperature.

observed (*data not shown*). The linear correlation between  $\ln(k_{\text{ex}})$  and  $1/T$  indicates the Arrhenius equation, and the slopes and  $y$ -intercepts of these lines yield the activation energies ( $\Delta G_0^\ddagger$ ) and Arrhenius constants ( $A$ ) of the hydrogen exchange process. All G imino protons have larger slopes ( $\Delta G_0^\ddagger = 28\text{--}30 \text{ kcal}\cdot\text{mol}^{-1}$ ) than those of the T imino protons ( $\Delta G_0^\ddagger = 16\text{--}19 \text{ kcal}\cdot\text{mol}^{-1}$ ). The larger activation energies of the G imino protons than the T imino protons indicate that the stable G-C base-pairs are more slowly exchanged with solvent water than the A-T base-pairs. In addition, the differences in the Arrhenius constants (indicating  $y$ -intercepts) within G/T imino protons are caused by the different equilibrium constants for the base-pair opening.

To further understand the dynamic property of the SPL14 consensus sequence DNA duplexes, the  $k_{\text{ex}}$  measurements in the three mutant SPL14 DNA duplexes were performed at 35 °C and then compared with those of the wt-SPL14. In the C4T-SPL14 duplex, where the C4-G23 base pair is changed to T-A base pair (*see* Fig. 1), the peak intensity of the T4 imino proton shows much larger dependence on the delay time after selective water inversion compared to the G23 imino proton of the wt-SPL14 duplex (Fig. 5(b)). This leads to a 16-fold larger  $k_{\text{ex}}$  value of the T4 imino proton than the

G23 imino proton in the wt-SPL14 duplex (Table 1), demonstrating that the A-T base pair is much less stable than the corresponding G-C base pair. Surprisingly, in the C4T-SPL14 duplex, the relative instability of the T4-A23 base pair induces the thermal stability of the neighboring T3-A24 base pair and the  $k_{\text{ex}}$  for the T3 imino proton has 3-fold smaller than that of wt-SPL14 duplex (Fig. 5(a)). This is consistent with 1D imino proton spectra of two duplexes, where the T3 imino proton of the C4T-SPL14 exhibits sharp resonance at 45 °C, whereas the corresponding resonance is clearly broadened in the wt-SPL14 (Fig. 1). However, there are no significant differences on the  $k_{\text{ex}}$  values between two duplexes for the G22 and G6 imino protons on the other side of the T4-A23 base pair (Table 1). These results indicate that the change from C4-G23 to T4-A23 base pair [indicating the 1 position of the consensus sequence (5'-C<sup>1</sup>C<sup>2</sup>G<sup>3</sup>T<sup>4</sup>A<sup>5</sup>C<sup>6</sup>R<sup>7</sup>-3')] in the wt-SPL14 duplex leads to destabilization of this base pair but significant stabilization of the neighboring base pair on only one side of the substitution.

Hydrogen exchange experiments were also performed at 35 °C for the G6A-SPL14 duplex, where the G6-C21 base pair is changed to A-T base pair (*see* Fig. 1). In the G6A-SPL14 duplex, the T21 imino proton has 3-fold larger  $k_{\text{ex}}$  value than the G6 imino proton of the wt-SPL14 duplex like the T4 imino proton in the C4T-SPL14 (Fig. 5(c) and Table 1). Surprisingly, the peak intensities of the neighboring T7 imino proton showed a weaker dependence on the delay time compared to the wt-SPL14 duplex (Fig. 5(d)), leading to a 2-fold smaller  $k_{\text{ex}}$  value of the T7 imino proton than that of the wt-SPL14 duplex (Table 1). The similar result was also observed on the  $k_{\text{ex}}$  value of the G22 imino proton on the other side of the A6-T21 base pair (Table 1). These results demonstrate that the change from G6-C21 to A4-T21 base pair [indicating the 3 position of the consensus sequence (5'-C<sup>1</sup>C<sup>2</sup>G<sup>3</sup>T<sup>4</sup>A<sup>5</sup>C<sup>6</sup>R<sup>7</sup>-3')] in the wt-SPL14 duplex leads to stabilization of two neighboring base pairs side of the substitution, although the A6-T21 base pair is slightly unstable than

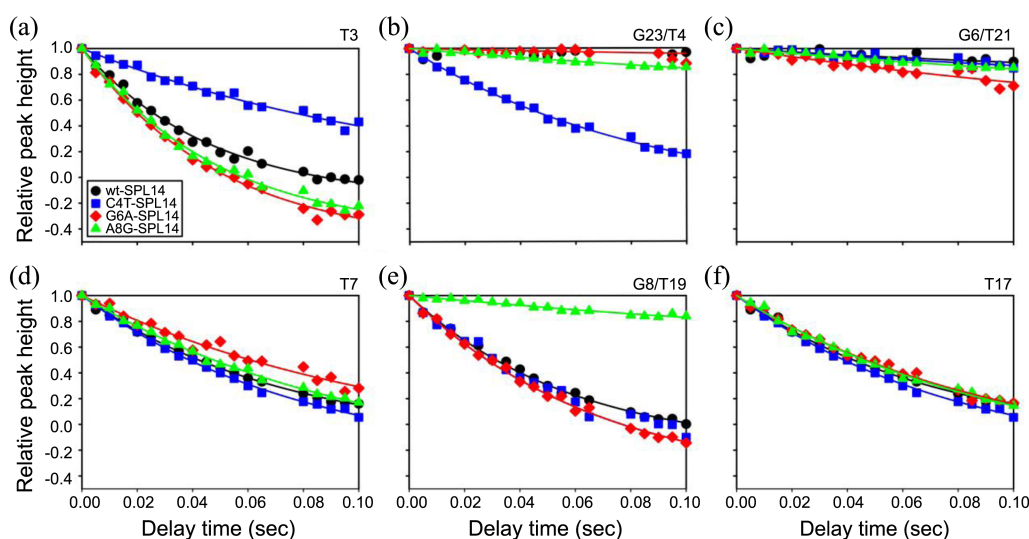


**Figure 5.** Relative peak height  $[I(t)/I_0]$  in the water magnetization transfer spectra for the (A) T3, (B) G23/T4, (C) G6/T21, (D) T7, (E) T19/G8, and (F) T17 imino protons of the wt- (circle), C4T- (square), G6A- (diamond), and A8G-SPL14 (triangle) duplexes as a function of delay time. Solid lines indicate the best fitting of these data using Eq. (1).

**Table 1.** Hydrogen exchange rate constants ( $s^{-1}$ ) of the imino protons for the wt-, C4T-, G6A-, and A8G-SPL14 duplexes at 35 °C

Imino	wt	C4T	G6A	A8G
G2	15.0 ± 3.9	16.1 ± 1.3	16.9 ± 1.7	14.7 ± 8.6
T3	19.6 ± 3.9	5.1 ± 1.2	18.9 ± 1.5	18.2 ± 2.0
G23/T4	0.5 ± 0.4	8.1 ± 0.8	0.3 ± 0.2	1.2 ± 0.7 <sup>b</sup>
G22	0.6 ± 0.5	0.5 ± 0.4	0.1 ± 0.1	1.3 ± 1.2
G6/T21	0.7 ± 0.6	0.9 ± 0.8	2.1 ± 1.4	1.2 ± 0.7 <sup>b</sup>
T7	11.5 ± 1.7 <sup>a</sup>	9.6 ± 0.6 <sup>a</sup>	6.6 ± 1.8	8.2 ± 1.2
T19/G8	14.7 ± 2.8	12.4 ± 1.8	13.5 ± 1.1	1.3 ± 0.8
G18	1.0 ± 0.4	0.8 ± 0.7	0.7 ± 0.6	1.2 ± 1.0
T17	11.5 ± 1.7 <sup>a</sup>	9.6 ± 0.6 <sup>a</sup>	8.5 ± 1.1	8.5 ± 1.4
G16	4.7 ± 0.9	3.6 ± 1.4	2.2 ± 1.8	4.2 ± 1.2

<sup>a</sup>The T7 and T17 resonances in the wt- and C4T-SPL14 overlap. <sup>b</sup>The G6 and G23 resonances in the A8G-SPL14 overlap.

the corresponding G6-C21 base pair in the wt-SPL14 duplex.

Hydrogen exchange rate constants of the imino protons for the A8G-SPL14 duplex, where the A8-T19 base pair is changed to G-C base pair (see Fig. 1), were also determined at 35 °C. The peak intensity of the G8 imino proton shows much smaller dependence on the delay time after selective water inversion compared to the T19 imino proton of the wt-SPL14 duplex (Fig. 5(e)). This leads to a 10-fold smaller  $k_{ex}$  value of the G6 imino proton than the T19 imino proton in the wt-SPL14 duplex as expected (Table 1). The neighboring T7 imino proton in the A8G-SPL14 duplex has slightly smaller  $k_{ex}$  value than that of the wt-SPL14 duplex (Fig. 5(d) and Table 1). However, there is no significant difference on the  $k_{ex}$  values between two duplexes for the G18 imino proton on the other side of the G8-C19 base pair (Table 1). These results demonstrate that the change from A8-T19 to G8-C19 base pair [indicating the 5 position of the consensus sequence (5'-C<sup>1</sup>C<sup>2</sup>G<sup>3</sup>T<sup>4</sup>A<sup>5</sup>C<sup>6</sup>R<sup>7</sup>-3')] also leads to destabilization of this base pair but stabilization of the neighboring base pair on only one side of the substitution.

The SELEX study revealed that AtSPL14 specifically recognizes core DNA-binding sequence (GTAC) with at least one additional flanking nucleotide.<sup>8</sup> Thus, the minimum consensus DNA sequence for effective AtSPL14-DNA interaction is thought to be 5'-C<sup>1</sup>C<sup>2</sup>G<sup>3</sup>T<sup>4</sup>A<sup>5</sup>C<sup>6</sup>R<sup>7</sup>-3' (where R is A or G).<sup>8</sup> EMSA competition assay study found that the C-to-A and C-to-T mutation at position 1 of the consensus sequence did not affect the DNA binding affinity of AtSPL14.<sup>8</sup> The two Zn-finger structures of the SBP domain bind to the consensus DNA sequence through the major groove of DNA duplex. The conformational change of the DNA duplex must occur during formation of the SBD-DNA complex for optimal binding between the Zn-finger structure and major groove of DNA duplex. It is thought to be that the conformational change is responsible for the binding affinity of the SBD to consensus DNA sequence. This study found that the C-to-T mutation at position 1 (C4T-SPL14 in this study) has no significant effects on the hydrogen exchange properties of the five consensus base pairs (5'-C<sup>1</sup>C<sup>2</sup>G<sup>3</sup>T<sup>4</sup>A<sup>5</sup>C<sup>6</sup>-3'). However, the point mutation at position 2-6 of the consensus sequence (5'-C<sup>1</sup>C<sup>2</sup>G<sup>3</sup>T<sup>4</sup>A<sup>5</sup>C<sup>6</sup>R<sup>7</sup>-3') significantly decreased the DNA binding affinity of AtSPL14.<sup>8</sup>

This hydrogen study found that, unlike C4T-SPL14, the G6A- and A8G-SPL14 duplexes showed the clear changes in the hydrogen exchange process of the five consensus base pairs (5'-C<sup>1</sup>C<sup>2</sup>G<sup>3</sup>T<sup>4</sup>A<sup>5</sup>C<sup>6</sup>-3'). Recently, the NMR study of methylated GATC DNA duplexes reported that the Gibbs free energy of the DNA conformation in the seqA-DNA complex could be estimated from the hydrogen exchange rate constants of the imino protons in the modified GATC DNA duplexes.<sup>14</sup> This Gibbs free energy the seqA-DNA complex can explain the unique feature of DNA binding affinity of the seqA protein.<sup>14</sup> Similarly, we can conclude that the unique dynamic features of the five base pairs in the consensus 5'-C<sup>1</sup>C<sup>2</sup>G<sup>3</sup>T<sup>4</sup>A<sup>5</sup>C<sup>6</sup>-3' sequence might play crucial roles in the effective DNA binding of the AtSPL14 protein.

In summary, we determined the  $k_{ex}$  values of the imino protons in the wild-type SPL14 consensus DNA sequence as well as the mutant DNA duplexes using NMR spectroscopy. The active C4T-SPL14 duplex has no significant effects on the hydrogen exchange properties of the five consensus base pairs at the position 5-9 on one side of this substitution. However, the inactive G6A- and A8G-SPL14 duplexes lead to clear changes in thermal stabilities of these five consensus base pairs. These unique dynamic features of the five base pairs in the consensus 5'-CGTAC-3' sequence might play crucial roles in the effective DNA binding of the AtSPL14 protein. Thus, this hydrogen exchange study can explain why the five conserved base pairs of the SPL14 binding site are very sensitive to substitution.

**Acknowledgments.** This work was supported by the National Research Foundation of Korea Grants [2010-0020480 and 2012-027750 (BRL)] funded by the Korean Government (MEST). This work was also supported by a grant from Next-Generation BioGreen 21 Program (SSAC, no. PJ009041), Rural Development Administration, Korea. We thank the GNU Central Instrument Facility for performing the NMR experiments.

## References

- Deyhle, F.; Sarkar, A. K.; Tucker, E. J.; Laux, T. *Dev. Biol.* **2007**, *302*, 154.
- Van Doorn, W. G.; Woltering, E. J. *Trends Plant Sci.* **2005**, *10*, 117.
- Groover, A.; Jones, A. M. *Plant Physiol.* **1999**, *119*, 375.
- Fukuda, H. *Plant Mol. Biol.* **2000**, *44*, 245.
- Gilchrist, D. G. *Annu. Rev. Phytopathol.* **1998**, *36*, 393.
- Beers, E. P.; McDowell, J. M. *Curr. Opin. Plant Biol.* **2001**, *4*, 561.
- Stone, J. M.; Liang, X.; Neel, E. R.; Stiers, J. J. *Plant J.* **2005**, *41*, 744.
- Liang, X.; Nazarene, T. J.; Stone, J. M. *Biochemistry* **2008**, *47*, 3645.
- Yamasaki, K.; Kigawa, T.; Inoue, M.; Tateno, M.; Yamasaki, T.; Yabuki, T.; Aoki, M.; Seki, E.; Matsuda, T.; Nunokawa, E.; Ishizuka, Y.; Terada, T.; Shirouzu, M.; Osanai, T.; Tanaka, A.; Seki, M.; Shinozaki, K.; Yokoyama, S. *J. Mol. Biol.* **2004**, *337*, 49.
- Yamasaki, K.; Kigawa, T.; Inoue, M.; Yamasaki, T.; Yabuki, T.; Aoki, M.; Seki, E.; Matsuda, T.; Tomo, Y.; Terada, T.; Shirouzu, M.; Tanaka, A.; Seki, M.; Shinozaki, K.; Yokoyama, S. *FEBS Lett.* **2006**, *580*, 2109.
- Delaglio, F.; Grzesiek, S.; Vuister, G. W.; Zhu, G.; Pfeifer, J.; Bax, A. *J. Biomol. NMR* **1995**, *6*, 277.
- Goddard, T. D.; Kneller, D. G. **2003**, SPARKY 3. University of California, San Francisco, CA.
- Lee, J.-H.; Pardi, A. *Nucleic Acids Res.* **2007**, *35*, 2965.
- Bang, J.; Bae, S.-H.; Park, C.-J.; Lee, J.-H.; Choi, B.-S. *J. Am. Chem. Soc.* **2008**, *130*, 17688.